

Lawrence Berkeley National Laboratory

LBL Publications

Title

Lattice and electronic structure of ScN observed by angle-resolved photoemission spectroscopy measurements

Permalink

<https://escholarship.org/uc/item/55s213sz>

Journal

Applied Physics Letters, 121(18)

ISSN

0003-6951

Authors

Al-Atabi, Hayder A

Zhang, Xiaotian

He, Shanmei

et al.

Publication Date

2022-10-31








DOI

10.1063/5.0119628

Peer reviewed

RESEARCH ARTICLE | NOVEMBER 02 2022

Lattice and electronic structure of ScN observed by angle-resolved photoemission spectroscopy measurements

Hayder A. Al-Atabi ; Xiaotian Zhang ; Shanmei He; Cheng chen ; Yulin Chen ; Eli Rotenberg ; James H. Edgar  

 Check for updates

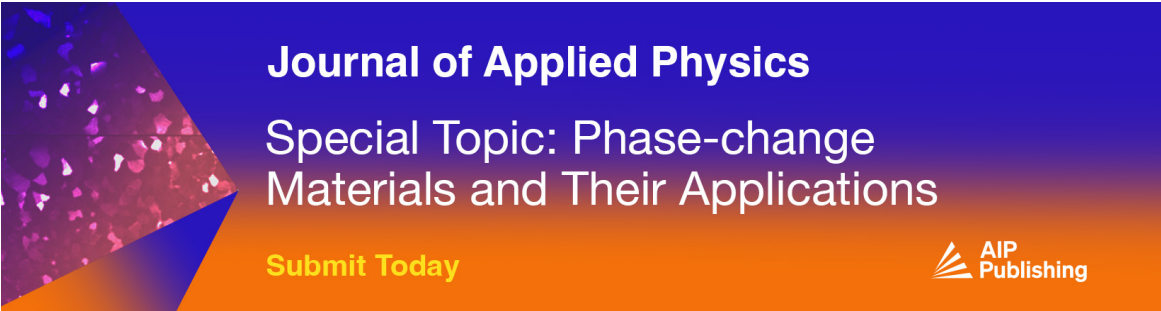
Appl. Phys. Lett. 121, 182102 (2022)

<https://doi.org/10.1063/5.0119628>

 CHORUS




CrossMark



Journal of Applied Physics
 Special Topic: Phase-change
 Materials and Their Applications

Submit Today



Lattice and electronic structure of ScN observed by angle-resolved photoemission spectroscopy measurements

Cite as: Appl. Phys. Lett. **121**, 182102 (2022); doi: [10.1063/5.0119628](https://doi.org/10.1063/5.0119628)

Submitted: 9 August 2022 · Accepted: 5 October 2022 ·

Published Online: 2 November 2022










View Online



Export Citation



CrossMark

Hayder A. Al-Atabi,¹  Xiaotian Zhang,^{2,3}  Shanmei He,⁴  Cheng chen,⁴  Yulin Chen,⁴  Eli Rotenberg,²  and James H. Edgar^{5,a)} 

AFFILIATIONS

¹Chemical Engineering Department, The University of Technology, Baghdad, Iraq

²Advanced Light Source, E.O. Lawrence Berkeley National Laboratory, Berkeley, California 94720, USA

³School of Mechanical Engineering, Shanghai Jiao Tong University, Shanghai, China

⁴Department of Physics, University of Oxford, Oxford OX1 3PU, United Kingdom

⁵Tim Taylor Department of Chemical Engineering, Kansas State University, Manhattan, Kansas 66506, USA

^{a)}Author to whom correspondence should be addressed: edgarjh@ksu.edu

ABSTRACT

Scandium nitride (ScN) has recently attracted much attention for its potential applications in thermoelectric energy conversion, as a semiconductor in epitaxial metal/semiconductor superlattices, as a substrate for GaN growth, and alloying it with AlN for 5G technology. This study was undertaken to better understand its stoichiometry and electronic structure. ScN (100) single crystals 2 mm thick were grown on a single crystal tungsten (100) substrate by a physical vapor transport method over a temperature range of 1900–2000 °C and a pressure of 20 Torr. The core level spectra of Sc $2p_{3/2,1/2}$ and N 1s were obtained by x-ray photoelectron spectroscopy (XPS). The XPS core levels were shifted by 1.1 eV toward higher values as the [Sc]:[N] ratio varied from 1.4 at 1900 °C to \sim 1.0 at 2000 °C due to the higher binding energies in stoichiometric ScN. Angle-resolved photoemission spectroscopy measurements confirmed that ScN has an indirect bandgap of \sim 1.2 eV.

Published under an exclusive license by AIP Publishing. <https://doi.org/10.1063/5.0119628>

Scandium nitride (ScN) is a group III nitride semiconductor with promising properties, which can overcome some limitations of conventional III–V compound semiconductors. It exhibits the rock salt crystal structure and octahedral bonding coordination.^{1–4} Due to its fundamental characteristics, which are not common in wurtzite III-nitride semiconductors or zinc blende III-arsenide semiconductors, ScN has recently attracted researchers' interest for its many different potential applications.⁵ It has been used as a substrate for producing high quality dislocation-free GaN,⁶ as a semiconductor in ZrN/ScN and TiN/(Al,Sc)N metal/semiconductor thermionic energy conversion devices,^{7–9} and as a semiconductor for thermoelectric energy conversion.^{10–12} Furthermore, an AlScN alloy is promising for 5G applications owing to its piezoelectric and ferroelectric properties.^{13–15}

ScN is mechanically hard (24 GPa hardness) and exhibits a high melting point of 2600 °C,^{16,17} which makes ScN suitable for refractory electronic and plasmonic applications. To study the electrical and compositional properties, several methods have been employed for growing ScN crystals such as hydride vapor phase epitaxy,¹⁶

molecular-beam epitaxy,¹⁸ magnetron sputtering,¹⁹ physical vapor transport (PVT) method in a resistively heated tungsten furnace,^{20,21} and other deposition methods.

Thin heteroepitaxial films are by far the most frequently studied form of ScN. An ultrahigh-vacuum reactive magnetron sputtering method was employed to grow epitaxial ScN on (001) MgO.²² The spectroscopic characterization and density functional theory calculations showed that ScN is a semiconductor with an indirect bandgap. ScN thin films utilizing rf molecular-beam epitaxy were deposited by Smith *et al.*¹⁸ Structural and elemental analyses revealed that the Sc/N flux ratio has a significant role in the stoichiometry and microstructure of ScN films. Nitrogen-rich conditions produced stoichiometric films, whereas Sc-rich conditions resulted in a sub-stoichiometric surface.

The surface roughness has a significant effect on the adatom mobility, which can affect the oxygen incorporation during growing ScN.²³ Moram *et al.*²⁴ deposited epitaxial ScN thin films with a cube-on-cube epitaxial relationship on a Si (100) substrate by molecular methods. The results revealed that the growth rate, surface roughness, and

crystalline quality are highly dependent on Sc flux rates. The surface roughness increased as the film thickness (>50 nm) increased because of the formation of square flat-topped islands due to the high growth rates and increasing grain sizes.

The electronic structure and characteristics of ScN have been extensively researched. In the electronic bonding of ScN, the scandium atom donates its two $4s$ electrons and single $3d$ electron to the nitrogen atom. In the rock salt structure of ScN, the five d levels of Sc couple with the three-valence p levels of nitrogen. The calculations of electronic densities of states showed that the nitrogen p states dominate the valence band of ScN, overlapping with a fraction of Sc d states, thus forming p - d states. The lowest conducting band is primarily anti-bonding $3d$ states of scandium. The bandgap arises from the separation of the bonding and nonbonding states.²⁵

Band structure calculations suggested that ScN is a semiconductor with an indirect bandgap (Γ -X) between 0.9 and 1.3 eV.^{22,26} The direct gap transition energies at X and Γ points were predicted to be 2.02 and 3.75 eV, respectively, based on hybrid functional Heyd-Scuseria-Ernzerhof (HSE06) calculations.²⁷ Experimentally, the X gap was detected between 1.26 and 3.2 eV,²⁷⁻³⁰ and the Γ gap was 4.25 eV.³¹

In our prior study of ScN produced by physical vapor transport, Hall-effect measurements indicated that ScN is n -type with an electron concentration and a mobility of $2.17 \times 10^{21} \text{ cm}^{-3}$ and $73 \text{ cm}^2/\text{V s}$, respectively. ScN crystal also has a low electrical resistivity of $3.94 \times 10^{-5} \Omega \text{ cm}$ and a thermal conductivity of $51\text{--}56 \text{ W/m K}$.²¹

Porte³² studied the electronic structures and the elemental composition of scandium nitride layers prepared by the reactive sputtering method. The x-ray photoelectron spectroscopy (XPS) analysis showed that the grown layers were a mixture of stoichiometric ScN and metallic scandium. The electron core levels Sc $2p_{3/2}$ were shifted by 1.5 eV higher binding energies (E_b) in the stoichiometric ScN ($E_b = 400.2 \text{ eV}$) than in the scandium metal ($E_b = 398.7 \text{ eV}$).

Haseman *et al.*²⁸ investigated the optical band of ScN grown by reactive magnetron sputtering and physical vapor transport methods employing cathodoluminescence and x-ray photoelectron spectroscopy techniques. Their results revealed that Sc $2p$ core levels shifted toward higher binding energies due to the presence of Sc-O bonds. Consequently, the oxygen incorporation was responsible for the degenerate doping and the shift in the optical (X - X) bandgap to 2.16 eV.

The present study was undertaken to more definitively determine the energy bandgap of ScN. Bulk single crystals of ScN (100) were grown via the physical vapor transport (PVT) method employing high growth temperature $\sim 2000^\circ\text{C}$. The lattice and electronic structure of bulk ScN crystals were measured via by angle-resolved photoemission spectroscopy (ARPES). This measurement had not previously been reported for ScN.

The physical vapor transport (also known as sublimation) growth of ScN crystals was conducted in a tungsten heating element furnace. The details are explained elsewhere.^{20,33} Tungsten does not appreciably react with nitrogen, thus tungsten crucibles, heating elements, and other furnace components are compatible for the sublimation crystal growth of ScN,³⁴ TiN,³⁵ and ErN.³⁶ In this case, it was also employed as a seed for the ScN crystals.

The single crystals of ScN were grown on a single crystal tungsten seed with a (100) orientation. The source of ScN was synthesized by

heating pure Sc metal (99.9% purity) in ultrahigh-purity nitrogen at 1100°C and 500 Torr for 10 h. The sublimation growth was carried out at temperatures ranging from 1900 to 2000°C with a nitrogen pressure of $15\text{--}20$ Torr.

The composition of the surfaces of the ScN samples was measured by x-ray photoelectron spectroscopy (XPS) employing a PHI 5000 VERSA PROB II. Prior to the measurements, the ScN crystal surfaces were clean by sputtering in helium to remove the oxygen and contaminations. The elemental composition of the ScN crystal was analyzed via Casa software.

In addition, we performed systematic ARPES experiments at Beamline 7 of the Advance Light Source to reconstruct the full band structures of the ScN crystal in the complete 3D Brillouin zone (BZ). For this purpose, the ScN single crystal, grown at 2000°C , was glued on a copper stage by Torr Seal epoxy, and a fresh surface of ScN single crystal was obtained by cleaving the crystal *in situ* under vacuum. The cleaved surface was maintained under UHV condition with pressure $<1 \times 10^{-10}$ Torr during the whole experiment. Photon energy-dependent ARPES measurements were then carried out within a photon energy range from 80 to 300 eV. The data were recorded with the total convolved energy and angle resolutions of 20 meV and 0.5° , respectively.

Figure 1 shows the core level spectra of Sc $2p_{3/2,1/2}$ and N $1s$ obtained by x-ray photoelectron spectroscopy (XPS) for ScN crystals grown at different temperatures. For ScN grown at 2000°C , the Sc $2p_{3/2}$ peak was at 400.5 eV, the Sc $2p_{1/2}$ peak at 405.2 eV, and the N $1s$ peak at 396.4 eV in agreement with the results reported by King *et al.*³⁷ The XPS core levels are shifted toward higher binding energies as the growth temperatures increase. The [Sc]:[N] ratio ranged from 1.4 at 1900°C growth temperature to approximately 1.0 at 2000°C . This is attributed to the greater molecular nitrogen reactivity, higher adatom diffusion rates, higher surface adatom mobility, and the suppression of the surface roughness, in which higher growth temperature produces less rough crystal surface.²⁰ However, these ratios are only estimates and could deviate slightly during the measurement or data analysis.

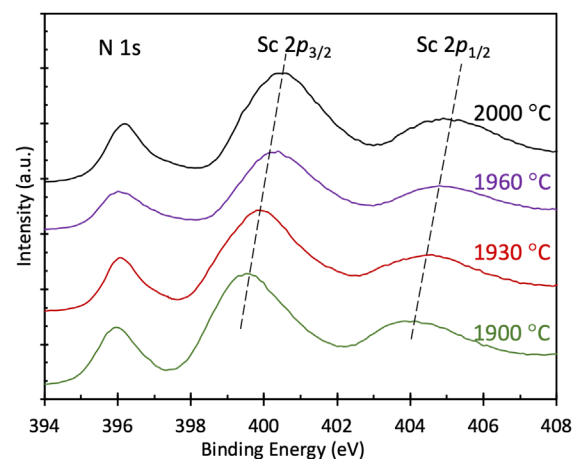


FIG. 1. Probing inhomogeneity of the crystal surface. X-ray photoelectron spectroscopy (XPS) for ScN crystals grown at different temperatures.

The shifting of the core levels of Sc $2p_{3/2,1/2}$ toward higher binding energies suggests that the non-stoichiometry layers grown at lower growth temperatures consist of two chemical entities, Sc metal and stoichiometric ScN. This result is in strong agreement with Porte,³² where the binding energies of Sc $2p$ spectra range from a value close to the metallic Sc to binding energies of stoichiometric ScN as the growth temperature is increased. In other words, due to higher adatom mobility resulted from higher growth temperature, N/Sc is increased, thus higher binding energies of Sc $2p$ core levels.

The XPS spectra did not reveal Sc peaks at 403 or 407 eV corresponding to Sc₂O₃. However, a small oxygen peak, 0.1–0.15 at. %, was detected. Most of this oxygen is believed to be limited at the surface of ScN crystals. As soon as sputtering step in XPS cleans the ScN surface, it immediately absorbs any oxygen present, even in an ultrahigh vacuum due to the extremely high affinity of Sc for oxygen. However, it is also possible that some level of oxygen, especially beyond the XPS detecting limit, exists in the body.

ARPES shows a series of in-plane (k_x - k_y) maps through the X point at different binding energies when the incident photon energy was set at 182 eV [Fig. 2(a)]. The top of valence bands at the X point reveals a fourfold symmetry, consistent with the point group of FCC ScN crystal [Fig. 2(b)]. A repeatable band features through Γ points appeared at photon energies of 116 and 268 eV indicating the neighboring Γ - Γ distance in the k_y direction is ~ 2.8 1/Å, which corresponds to a lattice constant of 4.5 Å in real space. We also noticed an electron pocket shows up at the X point, resulting from the n -type

behavior of the ScN crystal. Between the conduction band minimum (CBM) and valence band maximum (VBM), there is no signature of the in-gap states in any k_x , or k_y directions. Figure 2(c) demonstrates a band dispersion plot along Γ -X- Γ . The CBM located at ~ 0.4 eV below the Fermi level at the X point while the VBM was at ~ 1.6 eV Fermi level at the Γ point. These results confirm that the material preserves an indirect bandgap of ~ 1.2 eV. Interestingly, the conduction band at the X point in Fig. 2(d) shows an ellipsoidal shape in the k_x - k_y plane due to the distinct difference in effective mass between Γ -X and X-W directions. By fitting the dispersion of the pockets into a parabolic model, the effective mass m^* is estimated to be $0.9m_e$ along X-W and $0.2m_e$ along Γ -X.

The core level spectra of Sc $2p_{3/2,1/2}$ and N $1s$ obtained by x-ray photoelectron spectroscopy (XPS) for ScN crystals grown at different temperatures are shifted toward higher binding energies as the growth temperatures increase. This is due to the higher molecular nitrogen reactivity and higher adatom diffusion rates at higher temperatures. The non-stoichiometric layers grown at lower growth temperatures resulted in shifting the core levels of Sc $2p_{3/2,1/2}$ toward lower binding energies suggesting that the ScN crystals consist of two chemical entities, Sc metal and stoichiometric ScN. Angle-resolved photoemission spectroscopy (ARPES) measurements revealed that ScN has an indirect bandgap of ~ 1.2 eV, which is within the range of both theoretical and experimental previous studies.^{22,26} The Fermi level that is above the conduction band is indicative of degenerate n -type high electron concentrations. The conduction band at the X point showed an

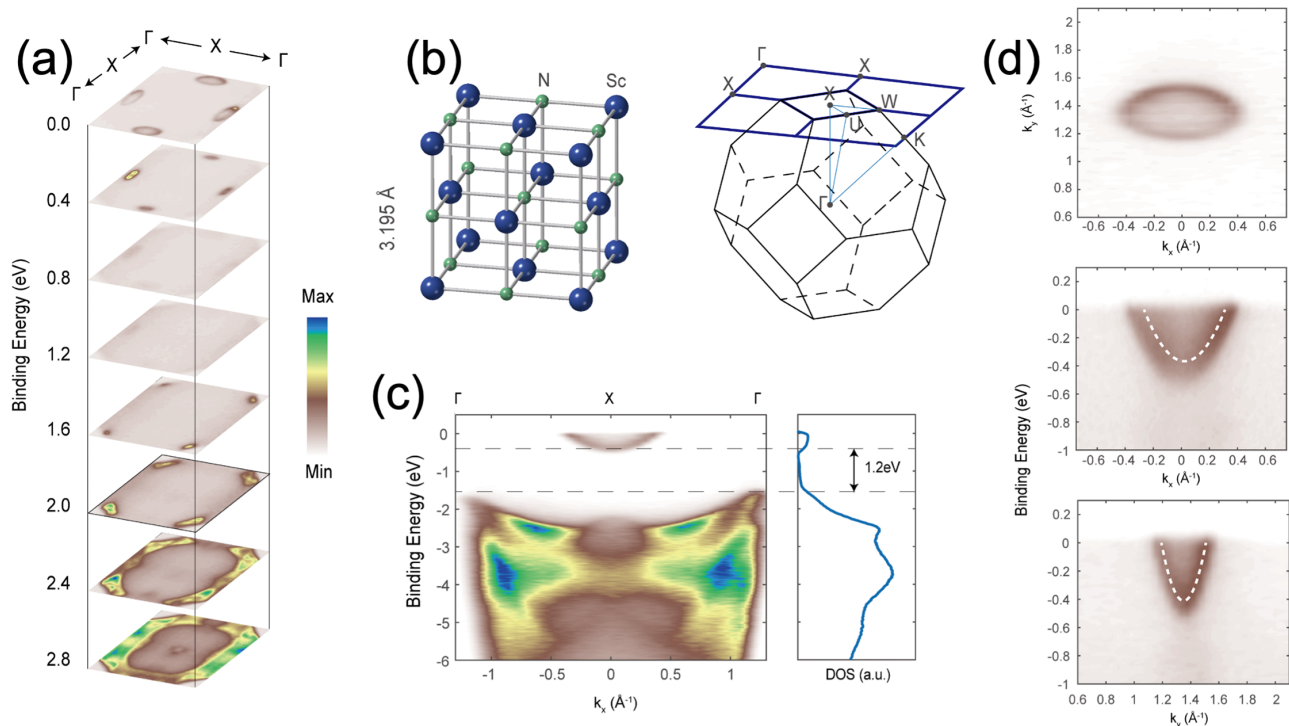


FIG. 2. (a) A series of constant energy contours through the X point at a photon energy of 182 eV. (b) Crystal structure of FCC ScN (left) and corresponding reciprocal structure in the Brillouin zone (right). (c) Band structure and DOS of ScN along Γ -X- Γ . (d) Fermi surface of the conduction band pocket projected onto the k_x - k_y plane (top) and the parabolic of the pockets in k_x (middle) and k_y (bottom) directions.

ellipsoidal shape in the k_x - k_y plane due to the difference in effective mass between Γ -X and X-W directions. The dispersion fitting of the parabolic model demonstrated that the effective mass is $0.9 m_e$ along X-W and $0.2 m_e$ along Γ -X.

H.A.A. and J.H.E. acknowledge the support for ScN crystal growth from the National Science Foundation under Grant No. DMR-1508172. This research used resources of the Advanced Light Source, a U.S. DOE Office of Science User Facility, as well as the Laboratory Directed Research and Development Program of Lawrence Berkeley National Laboratory, under U.S. Department of Energy Contract No. DE-AC02-05CH11231.

AUTHOR DECLARATIONS

Conflict of Interest

The authors have no conflicts to disclose.

Author Contributions

Hayder Abdulkareem Mohsin Al-Atabi: Conceptualization (equal); Investigation (equal); Methodology (equal); Visualization (equal); Writing – original draft (equal); Writing – review & editing (equal). **Xiaotian Zhang:** Conceptualization (equal); Data curation (equal); Formal analysis (equal); Investigation (equal); Methodology (equal); Writing – original draft (equal); Writing – review & editing (equal). **Shanmei He:** Conceptualization (equal); Data curation (equal); Formal analysis (equal); Investigation (equal); Methodology (equal). **Cheng Chen:** Conceptualization (equal); Data curation (equal); Formal analysis (equal); Investigation (equal); Methodology (equal). **Yulin Chen:** Conceptualization (equal); Formal analysis (equal); Investigation (supporting); Methodology (equal). **Eli Rotenberg:** Conceptualization (equal); Formal analysis (equal); Investigation (equal); Resources (equal); Writing – original draft (supporting); Writing – review & editing (supporting). **James Edgar:** Conceptualization (equal); Formal analysis (equal); Methodology (equal); Resources (equal); Supervision (equal); Writing – original draft (equal); Writing – review & editing (equal).

DATA AVAILABILITY

The data that support the findings of this study are available within the article.

REFERENCES

- B. Saha, J. Acharya, T. D. Sands, and U. V. Waghmare, *J. Appl. Phys.* **107**, 33715 (2010).
- A. Qteish, P. Rinke, M. Scheffler, and J. Neugebauer, *Phys. Rev. B* **74**, 245208 (2006).
- B. Saha, G. Naik, V. P. Drachev, A. Boltasseva, E. E. Marinero, and T. D. Sands, *J. Appl. Phys.* **114**, 63519 (2013).
- W. R. L. Lambrecht, *Phys. Rev. B* **62**, 13538 (2000).
- P. Eklund, S. Kerdsonpanya, and B. Alling, *J. Mater. Chem. C* **4**, 3905 (2016).
- M. A. Moram, Y. Zhang, M. J. Kappers, Z. H. Barber, and C. J. Humphreys, *Appl. Phys. Lett.* **91**, 152101 (2007).
- V. Rawat, Y. K. Koh, D. G. Cahill, and T. D. Sands, *J. Appl. Phys.* **105**, 24909 (2009).
- B. Saha, Y. R. Koh, J. Comparan, S. Sadasivam, J. L. Schroeder, M. Garbrecht, A. Mohammed, J. Birch, T. Fisher, and A. Shakouri, *Phys. Rev. B* **93**, 45311 (2016).
- M. Garbrecht, I. McCarroll, L. Yang, V. Bhatia, B. Biswas, D. Rao, J. M. Cairney, and B. Saha, *J. Mater. Sci.* **55**, 1592 (2020).
- S. Kerdsonpanya, N. Van Nong, N. Pryds, A. Žukauskaitė, J. Jensen, J. Birch, J. Lu, L. Hultman, G. Wingqvist, and P. Eklund, *Appl. Phys. Lett.* **99**, 232113 (2011).
- A. Shakouri, *Annu. Rev. Mater. Res.* **41**, 399 (2011).
- S. Kerdsonpanya, B. Alling, and P. Eklund, *J. Appl. Phys.* **114**, 73512 (2013).
- X. Liu, J. Zheng, D. Wang, P. Musavigharavi, E. A. Stach, R. Olsson, III, and D. Jariwala, *Appl. Phys. Lett.* **118**, 202901 (2021).
- X. Liu, D. Wang, K.-H. Kim, K. Katti, J. Zheng, P. Musavigharavi, J. Miao, E. A. Stach, R. H. Olsson, III, and D. Jariwala, *Nano Lett.* **21**, 3753 (2021).
- C.-Y. Chung, Y.-C. Chen, Y.-C. Chen, K.-S. Kao, and Y.-C. Chang, *Coatings* **11**, 1151 (2021).
- J. P. Dismukes, W. M. Yim, and V. S. Ban, *J. Cryst. Growth* **13–14**, 365 (1972).
- K. A. Gschneidner, *Rare Earth Alloys: A Critical Review of Alloy Systems of Rare Earth Scandium and Yttrium Metals* (Van Nostrand, 1961).
- A. R. Smith, H. A. H. Al-Brithen, D. C. Ingram, and D. Gall, *J. Appl. Phys.* **90**, 1809 (2001).
- D. Gall, I. Petrov, L. D. Madsen, J.-E. Sundgren, and J. E. Greene, *J. Vac. Sci. Technol. A* **16**, 2411 (1998).
- H. A. Al-Atabi, N. Khan, E. Nour, J. Mondoux, Y. Zhang, and J. H. Edgar, *Appl. Phys. Lett.* **113**, 122106 (2018).
- H. Al-Atabi, Q. Zheng, J. S. Cetnar, D. Look, D. G. Cahill, and J. H. Edgar, *Appl. Phys. Lett.* **116**, 132103 (2020).
- D. Gall, M. Städele, K. Järrendahl, I. Petrov, P. Desjardins, R. T. Haasch, T.-Y. Lee, and J. E. Greene, *Phys. Rev. B* **63**, 125119 (2001).
- A. Le Febvrier, N. Tureson, N. Stölkerich, G. Greczynski, and P. Eklund, *J. Phys. D* **52**, 35302 (2018).
- M. A. Moram, Z. H. Barber, C. J. Humphreys, T. B. Joyce, and P. R. Chalker, *J. Appl. Phys.* **100**, 23514 (2006).
- W. A. Harrison and G. K. Straub, *Phys. Rev. B* **36**, 2695 (1987).
- H. A. Al-Brithen, A. R. Smith, and D. Gall, *Phys. Rev. B* **70**, 45303 (2004).
- R. Deng, B. D. Ozsdolay, P. Y. Zheng, S. V. Khare, and D. Gall, *Phys. Rev. B* **91**, 45104 (2015).
- M. S. Haseman, B. A. Noesges, S. Shields, J. S. Cetnar, A. N. Reed, H. A. Al-Atabi, J. H. Edgar, and L. J. Brillson, *APL Mater.* **8**, 081103 (2020).
- T. Ohgaki, K. Watanabe, Y. Adachi, I. Sakaguchi, S. Hishita, N. Ohashi, and H. Haneda, *J. Appl. Phys.* **114**, 93704 (2013).
- J. More-Chevalier, S. Cichoń, L. Horák, J. Bulír, P. Hubík, Z. Gedeonová, L. Fekete, M. Poupon, and J. Lančok, *Appl. Surf. Sci.* **515**, 145968 (2020).
- J. More-Chevalier, S. Cichoń, J. Bulír, M. Poupon, P. Hubík, L. Fekete, and J. Lančok, *AIP Adv.* **9**, 15317 (2019).
- L. Porte, *J. Phys. C* **18**, 6701 (1985).
- H. A. Al-Atabi, M. I. Cheikh, M. H. Hosni, and J. H. Edgar, *Mater. Sci. Eng. B* **251**, 114443 (2019).
- Z. Gu, J. H. Edgar, J. Pomeroy, M. Kuball, and D. W. Coffey, *J. Mater. Sci.: Mater. Electron.* **15**, 555 (2004).
- L. Du, J. H. Edgar, E. A. Kenik, and H. M. Meyer, III, *J. Mater. Sci.: Mater. Electron.* **21**, 78 (2009).
- H. A. Al Atabi, Z. F. Al Auda, B. Padavala, M. Craig, K. Hohn, and J. H. Edgar, *Cryst. Growth Des.* **18**, 3762 (2018).
- S. W. King, R. F. Davis, and R. J. Nemanich, *J. Vac. Sci. Technol. A* **32**, 61504 (2014).